Microthermal Measurements at Karasu

Toshiyuki Sasaki, Norio Ohshima, Yoshitaka Mikami, Hisashi Koyanao, Michitoshi Yoshida, Yongqiang Yao, and Jun-Jie Wang

(reported by T. Sasaki on 2008-03-12)

ABSTRACT

Atmospheric turbulence is measured with microthermal sensors at 5 heights (36.65m, 19.15m, 10.15m, 6.25m and 4.15m) at Karasu during Oct 26 and 28, 2008. Microthermal measurements show that the surface turbulent layer affects below 19m high. Seeing sizes are estimated from microthermal measurements with an average of estimated seeing is 0.196 arcsec at ground level, larger than 0.1 arcsec observed at other observatory sites. Karasu site may be affected considerably with atmospheric turbulence triggered by mountain-lee-wave triggering mechanism.

1. Atmospheric turbulence estimated from microthermal measurements

The fluctuation in the refractive index of the air above the telescope affects the light path to degrade image of stars. The refractive index fluctuation is related to its thermal fluctuations. The refractive index variations arise from density variations in the air. Assumed that fluctuations are passive under the constant pressure, the refractive index variations arise directly from temperature fluctuations and can be measured by using the temperature fluctuations (Woolf 1982) with

$$C_n^2(z) = (7.9\ 10^{-5} \cdot P / T^2)^2\ C_T^2(z), \quad (1)$$

where C_n^2 is the refractive index structure coefficient, and C_T^2 the temperature structure coefficient. Pressure P is in hPa, temperature T in K degree, and z is height above ground in meter.

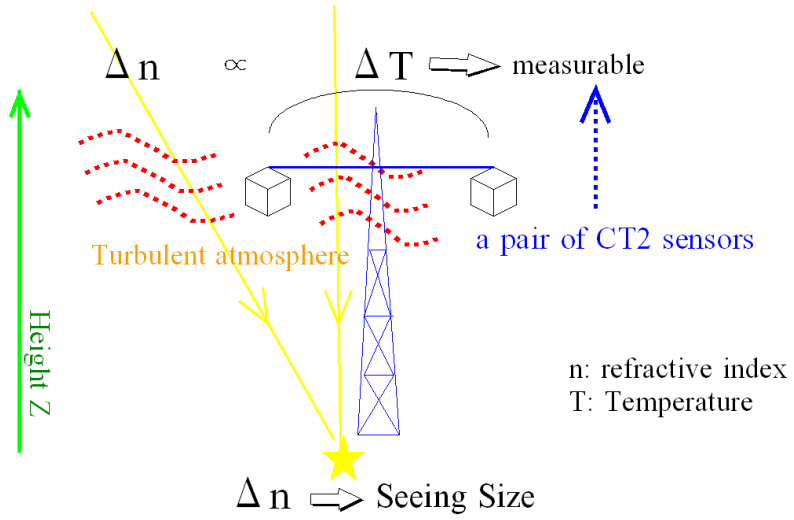

Figure 1. Concept to obtain seeing size by measuring temperature fluctuations.

A blurred image or seeing size is obtained by integrating the refractive index fluctuations along light path (Woolf 1982). As a wavelength-dependent length r_0, Fried's parameter (Fried 1982), is estimated (see details in Appendix 1),

seeing size θ (radian) is evaluated at full width at half maximum as

$$\theta(z) = 5.3\ \lambda^{-1/5} [\int_z^{\infty} C_n^2(z)\, dz]^{3/5}. \quad (2)$$

With the equation (1), we obtain the seeing size using temperature structure coefficient, C_T^2, as

$$\theta(z) = 5.3\ \lambda^{-1/5} (7.9\ 10^{-5} \cdot P / T^2)^{6/5} [\int_z^{\infty} C_T^2(z)\, dz]^{3/5}. \quad (3)$$

Within the context of observing quality, the microthermal structure of the surface boundary layer is of prime

importance (Erasmus 1986) as a significant portion of seeing degradation occurs in levels of the atmosphere close to the ground within a few tenths of meters above the ground. In the case of stratified air, we assume a vertical distribution of C_T^2 in exponential form with an exponential scale z_h as

$$C_T^2(z) = C_T^2(z_0) \exp\left(-(z-z_0)/z_h\right), \quad (4)$$

where $C_T^2(z_0)$ is the value at $z=z_0$. We obtain seeing at z as

$$\theta(z_0) = 5.3\,\lambda^{-1/5}\,(7.9\,10^{-5}\cdot P/T^2)^{6/5}\cdot(C_T^2(z_0)\cdot z_h)^{3/5} \quad \text{(radian)}. \quad (5)$$

Wyngaard et al. (1971) show that a vertical distribution of C_T^2 (z) obeys proportional to $z^{-4/3}$ under unstable atmospheric conditions and $z^{-2/3}$ under neutral cloudy conditions, but not clearly known in stable conditions (Kunkel & Walters 1981). We compare seeing estimations with these functional forms of C_T^2 vertical distributions to those with exponential form. Seeing distribution is obtained by integrating C_T^2 distribution functions, which are normalized at z=1m and an upper limit of integration is set of 100m in $z^{-2/3}$ case. Figure 2 shows vertical distributions of seeing with different functional forms of C_T^2 vertical distribution. In the $z^{-4/3}$ case for unstable conditions, seeing distribution presents close to one with an exponential distribution with a scale height of 5m and in the case $z^{-2/3}$ for neutral conditions nearly to with a scale height of 20m. As simplicity in integration, we use an exponential form of C_T^2 vertical distribution.

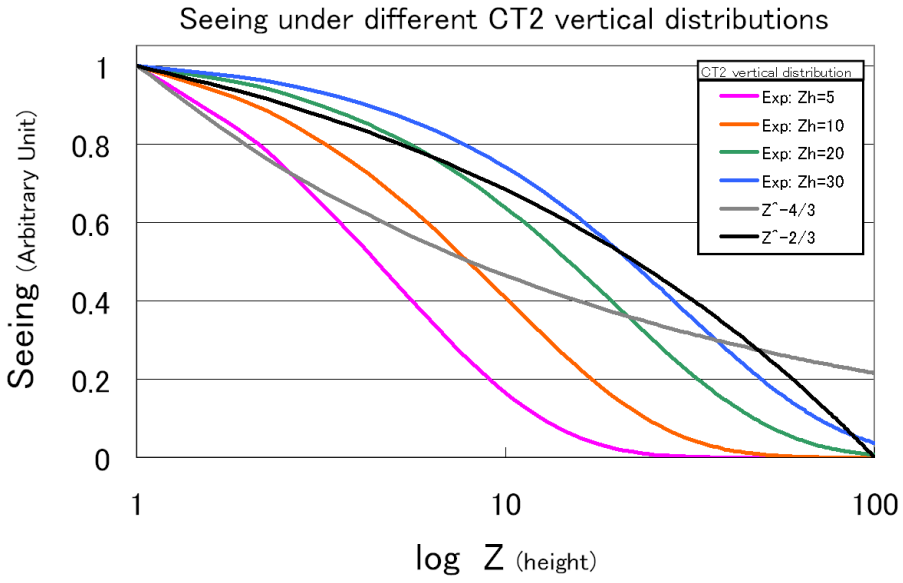

Figure 2. Comparison of seeing distributions estimated with different functional forms of C_T^2 vertical profile in $\exp(-z/z_h)$, $z^{-4/3}$, and $z^{-2/3}$.

2. Instruments for Microthermal measurement

The temperature structure coefficient, C_T^2, is defined as

$$C_T^2 = \langle |T(x) - T(x+r)|^2 \rangle \cdot r^{-2/3} \quad (K^2\,m^{-2/3}), \quad (6)$$

where r is a separation of two temperature sensors in meter. The microthermal measurements are made with resistance thermometers (Lynds 1964). Each thermometer consists of nickel wire of 25.4 μm thick and about 1.9 m long with their resistance of approximately 270 Ω (Figure 3).

A pair of CT2 sensors are attached to a support stay with temperature IC sensors (Figure 4 and 5). A separation of a pair of CT2 sensors is 1 meter apart. A total of 10 CT2 sensors on 5 support stays are installed on a 40 m tall tower at Karasu (Figure 10). A temperature sensor, AD590MH (Analog Devices), is attached near the center of each stay. An addition support hangs a barometer, Vaisala PTB210 as shown in Figure 5 and 10.

On the CT2 sensors the nickel wire is acting as temperature-sensitive resistance in a bridge circuit operated with 7.5V, giving a sensitivity of approximately 5 mV/degree using a circuit board for CT2 sensors (Figure 6). The current passing the CT2 sensors is about 4.2 - 4.3 mA. The voltage difference of CT2 sensors is about 5 mV.

The output from the bridge circuit is amplified by 1000 and filtered to pass signals with 0.8Hz to 35 Hz (Figure 7).

Figure 3. CT2 sensor spiral-bound with a thin nickel wire of 25.4 μm thick and about 1.9 m long. Resistance is kept about 270 Ω within ±3.0 Ω. The mesh guard is for protecting the nickel wire. Base plates are made of acrylic resin and four supporting rods of Delrin.

Figure 4. A pair of CT2 sensors are attached to a support stay at left and right end. The separation is 1 m apart. A temperature IC sensor, AD590MH (Analog Devices), is installed close to the center of the stay.

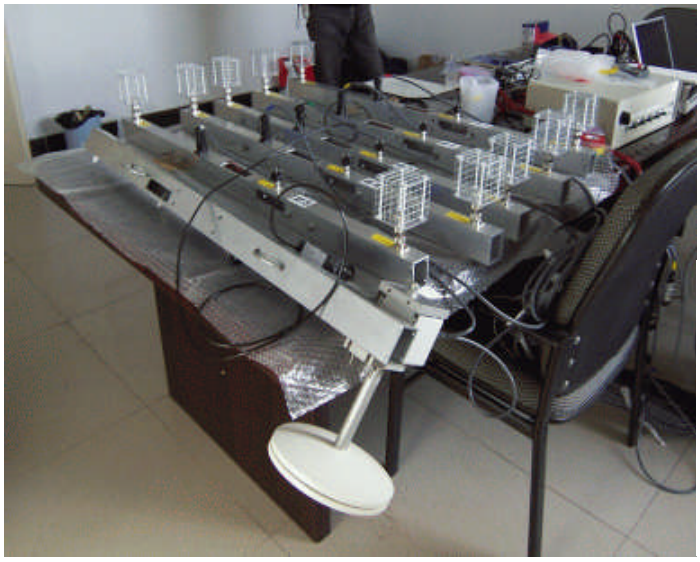

Figure 5. A total of 10 CT2 sensors on 5 support stays and an addition support hanging a barometer, Vaisala PTB210. An electric box, seen left to the stays, is a controller for CT2 sensors.

With a RMS-DC IC (National Advances AD536ASD), amplified differential voltages of CT2 sensors are measured to get their root mean square (rms) values. An output range of AD536ASD is 0 to 7V when voltage supply to AD536ASD is ±15V. In the case of one of the wires on paired CT2 sensors is broken, a voltage difference as much as input voltage of amplifier, 15 V, is input to AD536ASD, then false rms should be measured about 7 V. From the datasheet of AD536ASD, a settling time to measure the rms voltage with AD536ASD using a bandpass filter (Fig.6) is around 100 msec in the case of its measurement error of 1%. We measure C_T^2 values with longer time of 5 seconds to get higher accuracy. A system offset level is measured using a constant resistance instead of CT2 sensors under temperature-controlled environment at the laboratory at Mitaka, and its values are obtained around 1.5 mV which corresponds to C_T^2 level of 7.4 10^{-8} $K^2m^{-2/3}$, although a datasheet of AD536ASD describes its maximum total error of ±3 mV ± 0.3% of its reading (3 mV corresponds to C_T^2 error of 3.33 10^{-7} $K^2m^{-2/3}$). A data acquisition system or digital multimeter (DMM), KEITHLEY Integra 2701 with I/O card 7702, is used to digitize rms voltages which transfer to PC via Ethernet connection (Fig. 8 and 9). On PC, C_T^2 values are calculated from rms voltages.

As shown in Appendix 2, conversion of differentail voltages of paired CT2 sensors to temperature differences is obtained as

$$\Delta V / \Delta T = -V_C R_D C_T / (R_{273} + C_T (T(K) - 273.15) + R_D)^2, \quad (7)$$

where V_C is a supply voltage to the bridge circuit, R_D a constant resistance in the bridge, C_T resistance dependency on temperature, R_{273} is the resistance of the nickel wire at 0 ℃ we used, and T(K) temperature in K degree. Then a conversion factor f_{conv} to a C_T^2 value from rms of amplified voltage difference, V_{rms}, measured with AD536ASD is obtained as

$$f_{conv}(T, \Delta T) = (R_{273} + C_T (T(K) - 273.15) + R_D)^4 / (1000 \times V_C R_D C_T)^2. \quad (K^2 m^{-2/3} V^{-2}) \quad (13)$$

Typical values of $f_{conv}(T, \Delta T)$ are 0.0364, 0.0370, and 0.0394 at -5, 0 and 20 ℃, respectively. Taking into account an offset voltage, V_{offset}, by AD536ASD, then we obtain C_T^2 values from V_{rms} as

$$C_T^2 \text{ value} = f_{conv}(T, \Delta T) \times (V_{rms} - V_{offset})^2. \quad (14)$$

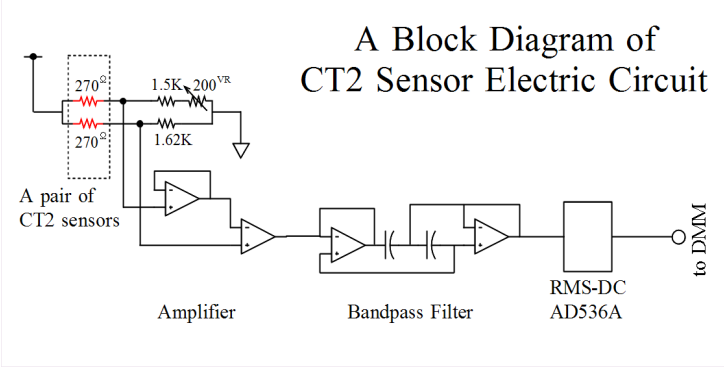

Figure 6. A block diagram of CT2 circuit, where input signals from a pair of CT2 sensors are amplified, applied with a band-pass filter, then measured their rms values using RMS-DC IC, AD536ASD (Analog Devices).

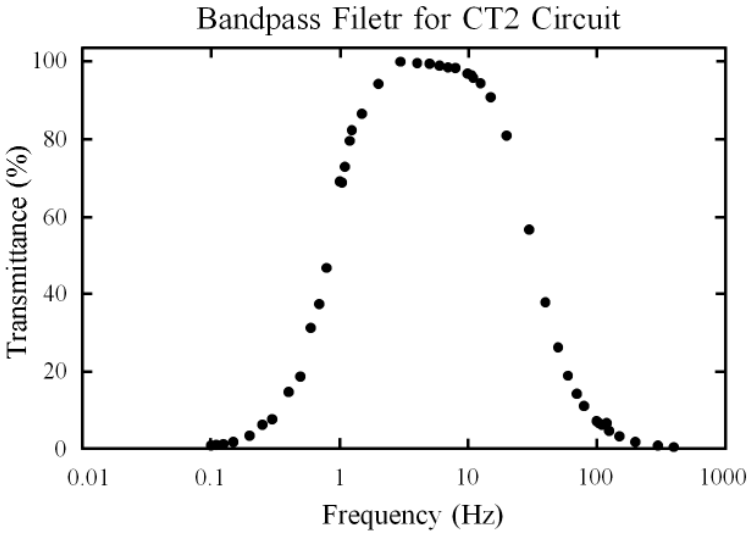

Figure 7. Transmittance of a band-pass filter for CT2 circuit with 50% transmittance at 0.8 Hz and 35 Hz.

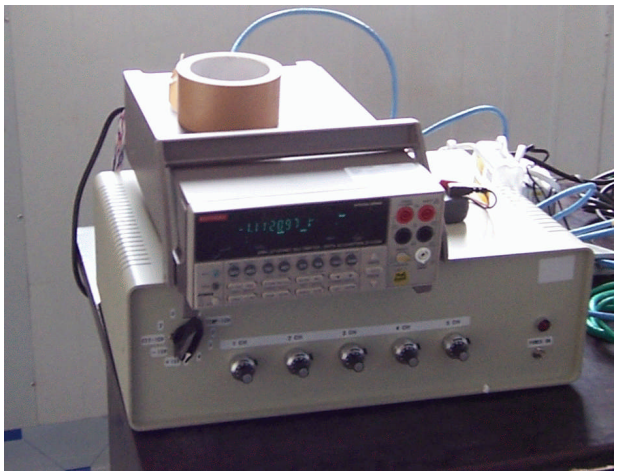

Figure 8. A control box (below) contains the circuit board for CT2. Above the control box is a data acquisition system, KEITHLEY Integra 2701 with I/O card 7702, which digitize voltages and transfer them to PC via Ethernet connection.

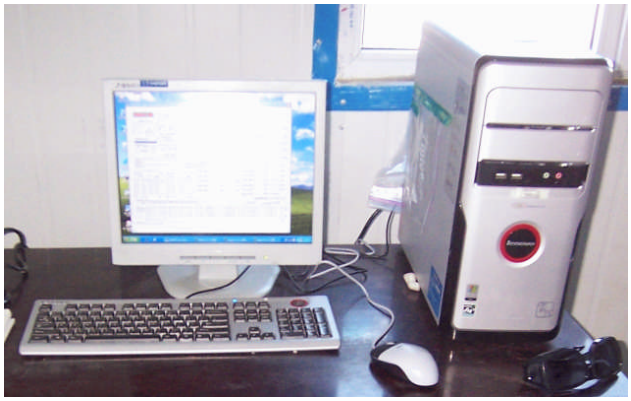

Figure 9. A PC runs a control software and utility software to control, take and display C_T^2 measurements.

The temperature sensor, AD590MH (Analog Devices), measures temperature at 10 mV / 1° with the working range of -55℃ to +150℃. Its temperature resolution is about 0.01° coupled with DMM resolution of 100μV. The barometer, Vaisala PTB210, measures atmospheric pressure in the range of 500 hPa to 1100 hPa with its output voltage in 0 V to 5 V, respectively, with resolution of 300μV. As its working temperature is of -40 to +60 ℃, an air entrance is protected against accumulation of frosts and/or ices by being heated at lower temperature than +4 ℃.

3. Installation of Microthermal CT2 Sensors at Karasu

A total of 10 Microthermal CT2 Sensors are installed on a 40 m-tall tower at Karasu at 5 levels of 36.15m, 19.15m, 10.15m, 6.25m and 4.15m above ground (Fig. 10). A temperature sensor is installed at each level. One additional level is selected to hang the barometer, Vaisala PTB210, at 2.65m high. At the foot of the tower, the electric control

Figure 10. The 40m weather tower with CT2 sensors and temperature sensors at 36.65m, 19.15m, 10.15m, 6.25m, and 4.15m, and the barometer at 2.65m. (Left) The lowest stay hangs the barometer and other two keep a pair of CT2 sensors and a temperature sensor.

box and the DMM are set in a small protected box. The control PC sits in an observing house about 40m apart from the tower and an Ethernet cable and a power line are set up by digging the ground.

4. Microthermal measurements and seeing estimated at Karasu

Microthermal measurements were conducted during Oct 26 and 28, 2008. C_T^2 values are shown in Fig. 11. Their histogram is shown in Fig. 12, indicating that turbulance is stronger below 19 m above the ground, where might locate above a turbulent surface layer. As wind speeds were around 7-9 m/sec on these days, a small hill on the windward side (toward west) affects Karasu site with additional surface turbulence induced by the hill.

To estimate seeing size, we assume a vertical distribution of C_T^2 in exponential form with a scale height z_h following Miyashita et al. (1989) and Wada et al. (2004) as

$$C_T^2(z) = C_T^2(0) \exp(-z / z_h), \quad (15)$$

where $C_T^2(0)$ is the value at the ground level z=0. By fitting to a vertical distribution of measured C_T^2 values we obtain a scale height z_h at first. Then seeing sizes at five levels corresponding to CT2 sensors and the ground level are estimated as described in Appendix 1,

$$\theta(z) = 5.3\,\lambda^{-1/5}\,(7.9\,10^{-5} \cdot P / T^2)^{6/5} \cdot (C_T^2(z) \cdot z_h)^{3/5}. \quad \text{(radian).} \quad (16)$$

Figure 13 shows the distribution of seeing estimated at ground and at five layers. Following the equation (16), seeing in the range of z1 to z0 is calculated as

$$\theta(z_1{:}z_0) = (-\theta(z_1)^{5/3} + \theta(z_0)^{5/3})^{3/5}, \quad \text{(radian).} \quad (17)$$

where z_0 is set to the highest height of 36.65m.

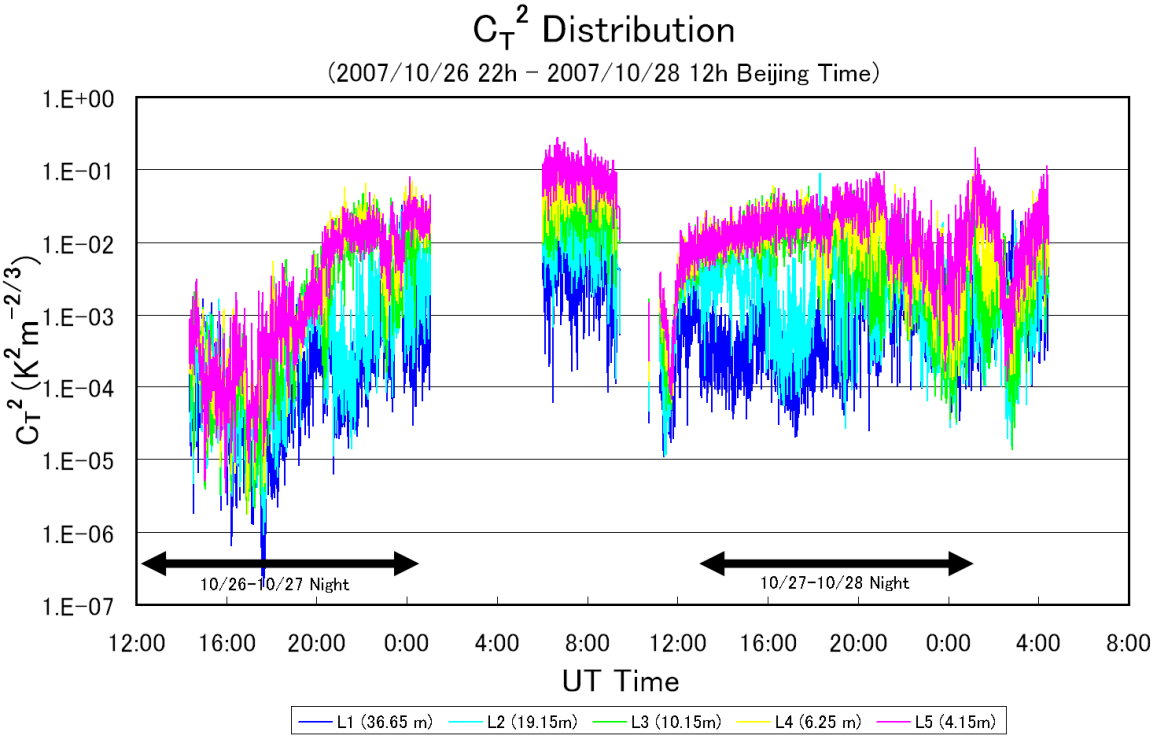

Figure 11. C_T^2 distribution measured during Oct 26 and 18, 2008 at Karasu. It was cloudy at Karasu early night on Oct 26 and after then it was clear.

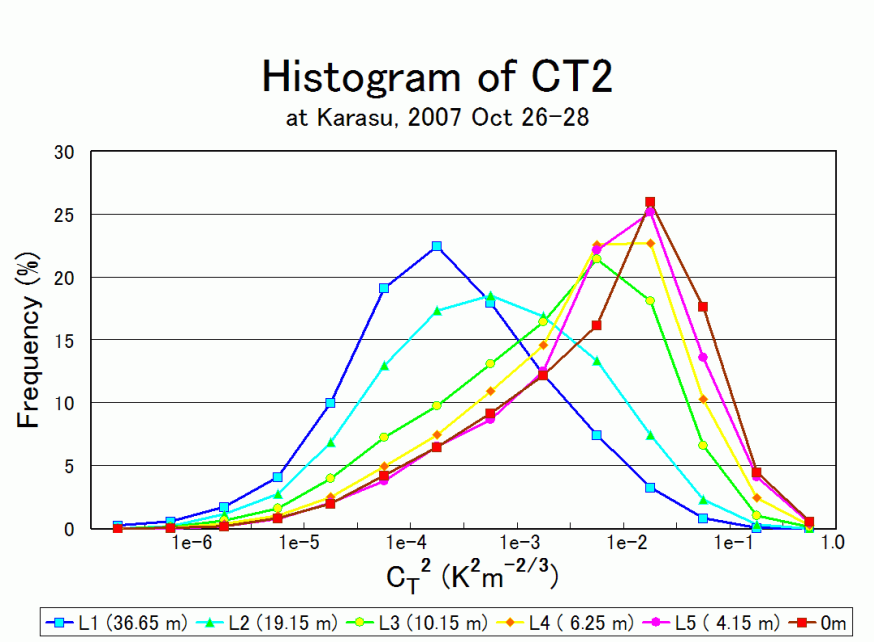

Figure 12. Histogram of C_T^2 values measure during night on Oct 26 and 28,

Seeing distributions are obtained between maximum height of 37 m and other lower heights to show their histogram during night (UT 13:00 – UT 01:00) in Figure 14. A relatively large seeing was observed lower than 19 m. Average seeing values are presented in Table 1. In calculating seeings, we used measurements of atmospheric pressure and temperatures. An average Pressure is observed of 595.5 hPa with its range of 594.3 hPa (min) to 596.8 hPa (max) and an average temperature of 267.187 K with its range of 263.093K (min) to 272.332K(max).

Table 1. Average seeing in vertical ranges of measurements during observation nights

Range	Average seeing
37 m - 19m	0.069 arcsec
37 m - 10 m	0.123 arcsec
37 m - 6 m	0.142 arcsec
37 m - 4 m	0.166 arcsec
37 m - ground	0.196 arcsec

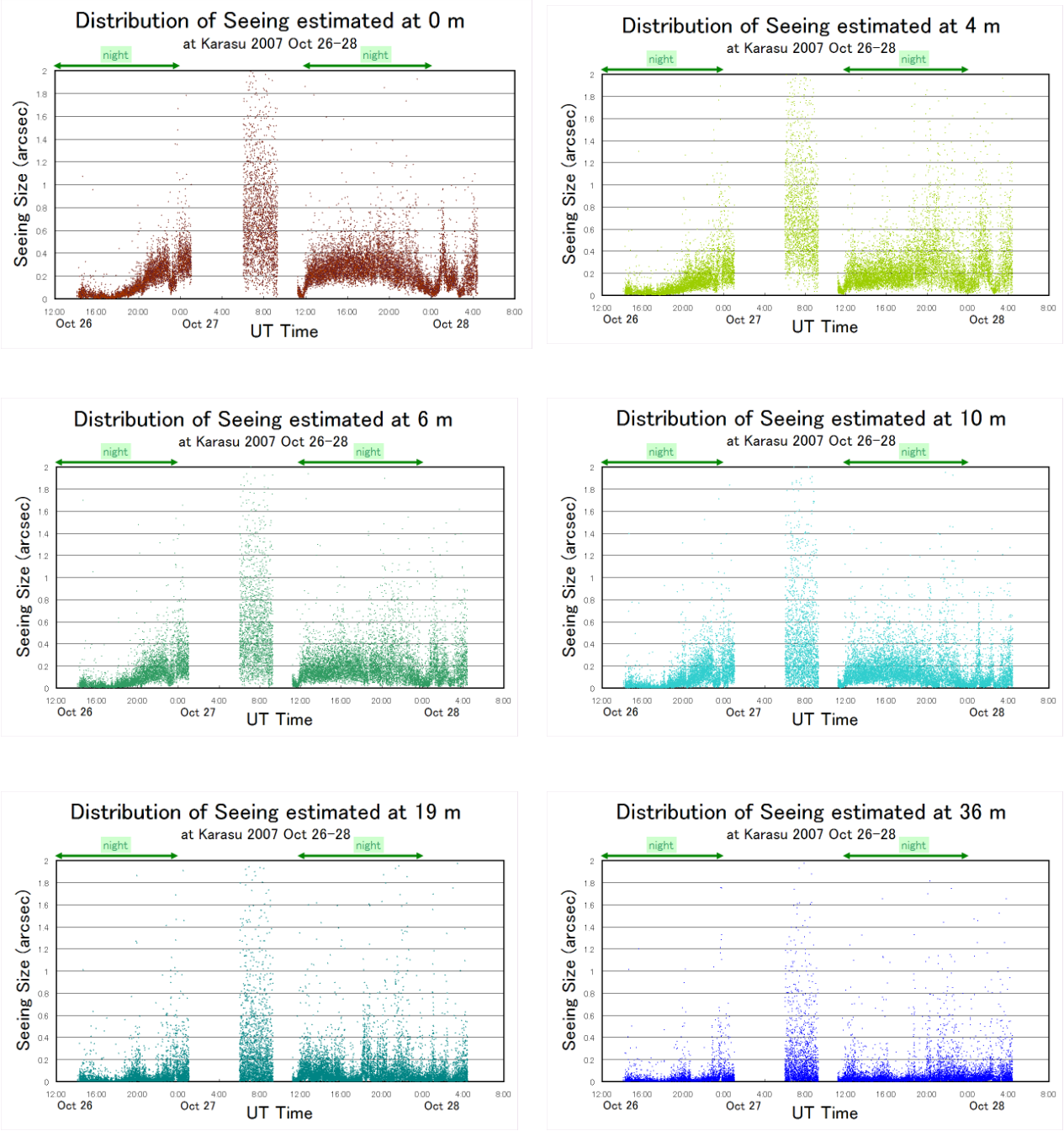

Figure 13. Seeing distributions estimated at 0 m, 4 m, 6 m, 10 m, 19 m, and 37 m during Oct. 26 and 28, 2008 at Karasu..

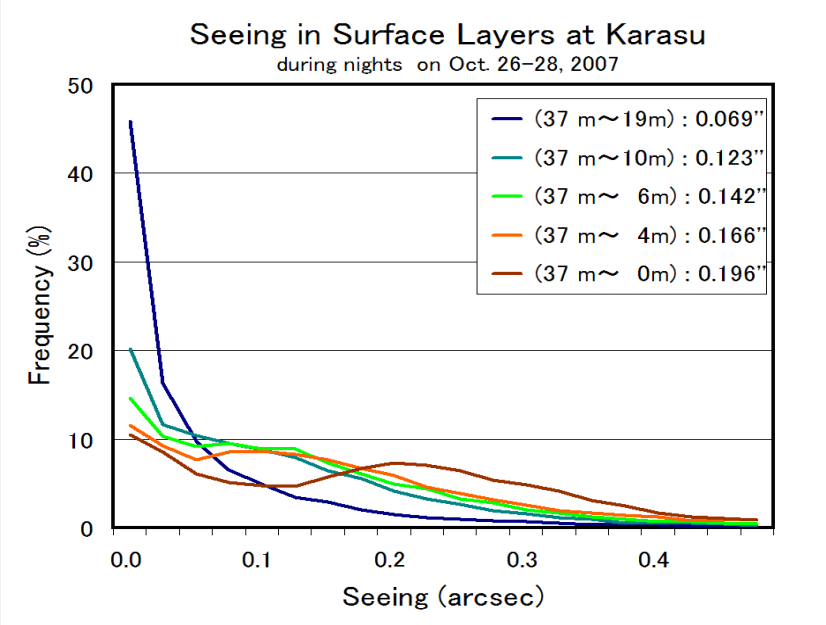

Figure 14. Histogram of seeing in the vertical ranges of measurements at Karasu during nights on Oct. 26-28, 2008.

Scale heights of the exponential form of C_T^2 vertical distribution are obtained by fitting the measurement by the least square method and their histogram is shown in Figure 15. An average scale height is around 11 m and a mode of scale heights about 6 m during nights on Oct. 26 – 28, 2008. Seeing sizes above 19m high might be decreased to 35 % ($\sim \exp(-19/11)$)$^{3/5}$) of those at the ground level. In our estimation of seeing with C_T^2 vertical distribution in exponential form, a practical limitation of integration occurs around $4.6Z_h$. That is, our seeing estimations may give reasonable values in the case of Z_h less than 8 m in our measurements where the highest level of CT2 sensors is 37 m.

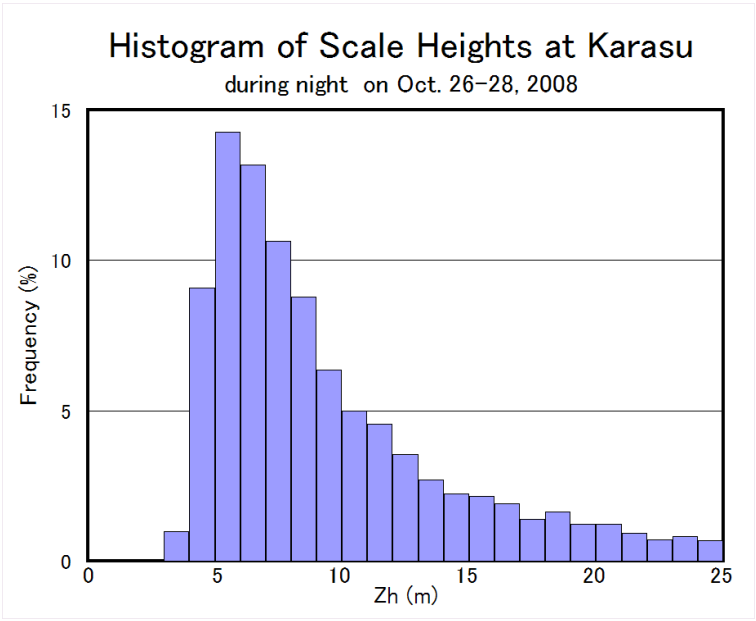

Figure 15. Histogram of scale heights, Z_h, for vertical distribution of C_T^2 in exponential form during observation nights.

5. Comparison of Microthermal measurements at Okayama and at Karasu

At Okayama Astrophsical Observatory (OAO, Japan) seeing measurements have been conducted to evaluate the

site for their new 3.5 m telescope (Wada et al. 2004). We have compared our CT2 sensor system to those used at OAO. Electric systems are almost the same, but sensors and software systems are different. A 27 m tower at Okayama was used to install our CT2 sensors at five heights and OAO's CT2 sensors at four heights. A top layer and 2nd layer hang both CT2 sensor pairs at the same heights, and others at separate heights. By the relatively strong wind, some OAO sensors were broken, but alive CT2 sensors at the highest level were used to compare C_T^2 values with each CT2 system. Both C_T^2 data show to match to each other almost completely as shown in Figure 16. Some discrepancy was observed at low C_T^2 values below 1.3 10^{-5} $K^2m^{-2/3}$. This discrepancy may be caused partially due to subtraction of offsets of AD536ASD, that is, offset voltages are subtracted in converting V_{rms} to C_T^2 in our system and not in OAO system. For example, when V_{rms} is 3 mV, C_T^2 is calculated as 8.3 10^{-8} $K^2m^{-2/3}$ with offset subtraction of 1.5 mV and 3.3 10^{-8} $K^2m^{-2/3}$ without the subtraction. But the discrepancy between them is much larger as C_T^2 of 1.3 10^{-5} $K^2m^{-2/3}$ corresponds to V_{rms} of 18mV. The cause of this discrepancy is still unknown.

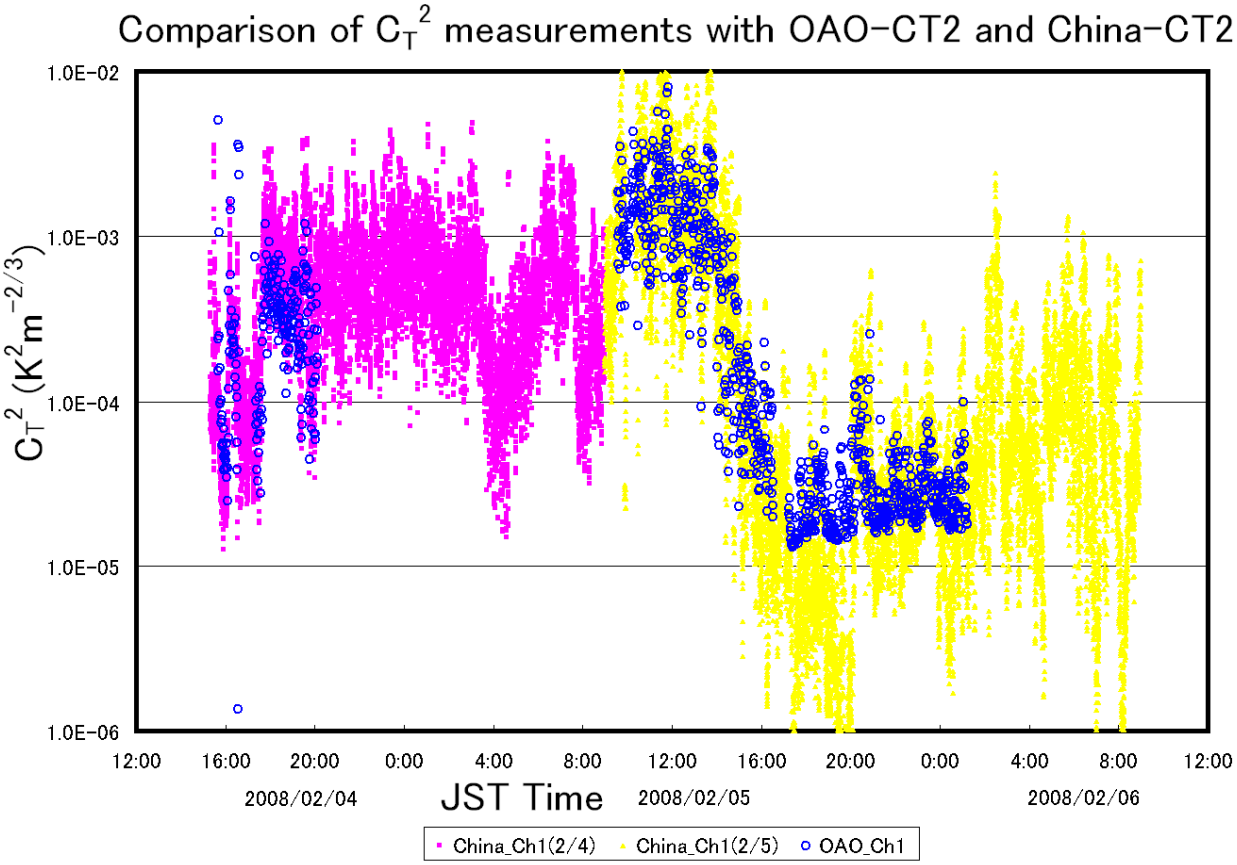

Figure 16. Comparison of C_T^2 measurements at OAO with CT2 system of OAO and of ours taken on Feb. 4 and 6, 2008. Almost the same measurements were obtained for the data taken at highest level. Some discrepancy was observed at C_T^2 lower than 1.3 10^{-5}.

Seeing were obtained from C_T^2 measurements at OAO during 12:00, Feb.5 2008 to 9:30, Feb.6 2008 as the nickel wire on one of CT2 sensors was loosened to fail in working correctly on the first day. Seeing distribution is shown in Figure 17. An average seeing at ground level was estimated as 0.04 arcsec (Figure 18). Scale heights of exponential distribution of C_T^2 are shown in Figure 19. A mode of the scale heights was around 7.5m. The atmospheric pressure was observed of 977.5 hPa and the average temperature of 276.2 K with its range of 272.1K (min) and 281.4K (max).

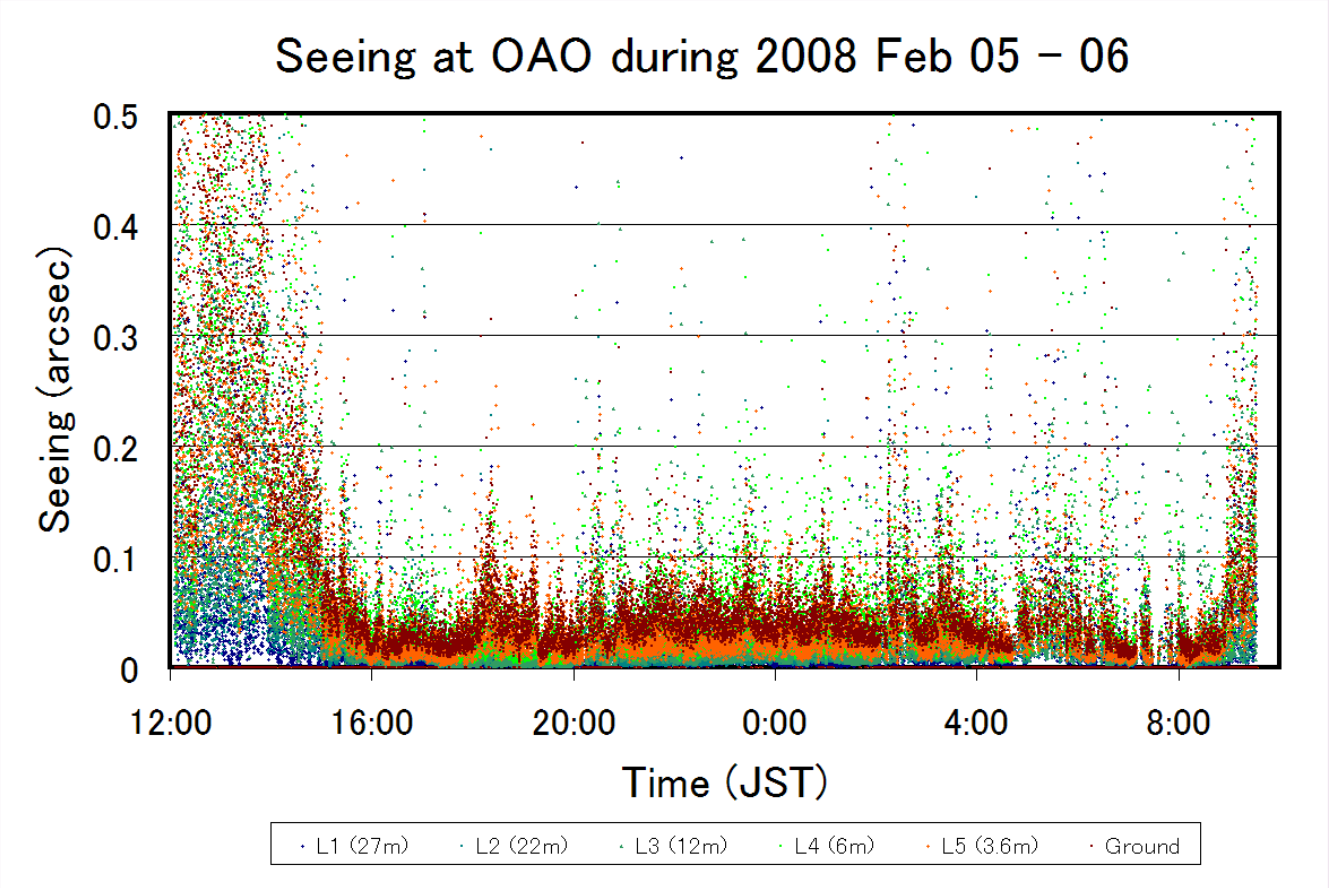

Figure 17. Seeing distribution estimated at OAO during 12:00, Feb.5 2008 to 9:30, Feb.6 2008. Abscissa is time in Japan Standarad Time (JST).

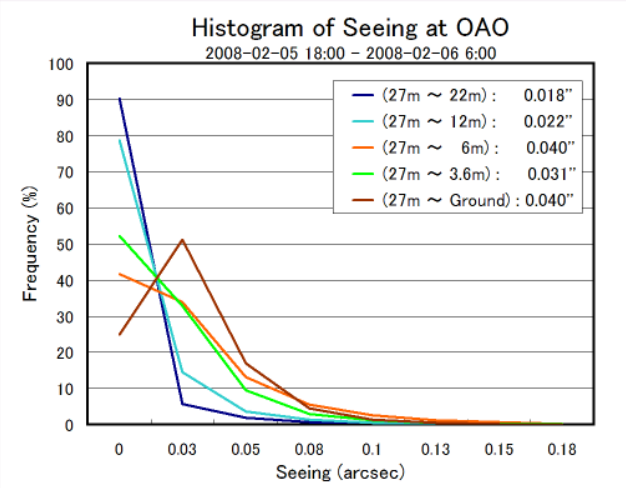

Figure 18. Histogram of seeing distribution at OAO during 18:00, Feb. 5 to 6:00, Feb. 6 2008 (JST).

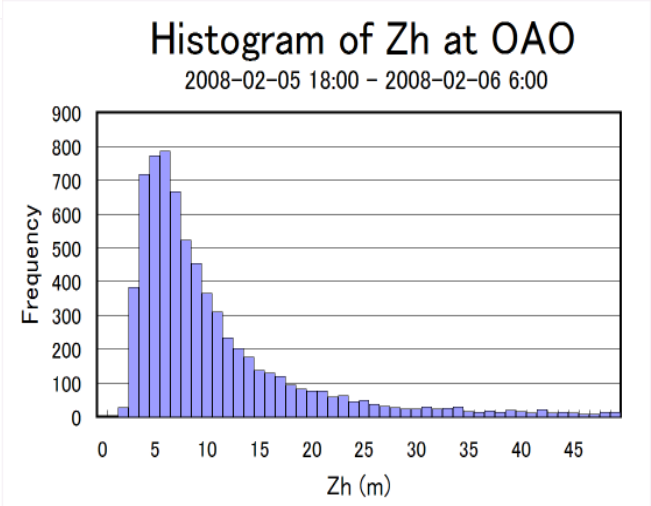

Figure 19. Histogram of scale heights of C_T^2 exponential distribution at OAO during 18:00, Feb. 5 to 6:00, Feb. 6 2008 (JST).

6. Discussions and Future plans

Microthermal C_T^2 measurements were conducted successfully at Karasu and our CT2 system worked well. By

comparing with C_T^2 measurements using OAO CT2 system and ours at OAO, the C_T^2 measurements can be pronounced to be confirmed. Seeing estimation is carried on under assumption of the exponential vertical distribution of C_T^2 values instead of $z^{-4/3}$ or $z^{-2/3}$ proposed for unstable/neutral turbulent layers (Wyngaard et al. 1971). The assumption of the exponential vertical distribution cannot introduce large errors in estimated seeing.

Average seeing values were obtained at Karasu of 0.196 arcsec at the ground level and 0.166 arcsec at 4m. These are considerably larger compared to 0.040 arcsec at the ground and 0.031 arcsec at 3.6 m, observed at OAO during night on Feb. 5-6, 2008. Contribution of seeing induced by surface turbulent layer is around 10-15% of total seeing measured with DIMM (Martin et al. 2000 at Paranal(Chile) and Sanchez at al. 2003 at San Pedro Martir). Equivalent seeing contributions of the surface layer are calculated less than 0.1 arcsec between 3m and 21m above the ground at Paranal and around 0.1 arcsec between 2.3m and 15m at San Pedro Martir.

As Karasu site is surrounding high mountains and a small hill locates windward (to the west), turbulence may be triggered considerably at Karasu due to a mountain-lee-wave triggering mechanism (Bufton 1973). As a geographical research for site selection is the first step to select the site candidate to settle astronomical telescopes, turbulent effects induced by mountains and even by a small hill windward must be taken into consideration in selecting candidate sites.

As continuous monitoring on site characteristics through a year is important, we conduct continuous measurements at Karasu, Oma and other candidate sites around Hami (Sasaki 2008) at least through one year. Simultaneous observations of seeing using DIMM and MASS are desirable and mandatory to evaluate the sites for astronomical use. DIMM shows integral characteristics through the light path which is affected by atmospheric turbulences to cause natural seeing. MASS can measure turbulence strengths in several layers higher in the atmosphere. Microthermal C_T^2 measurements show the behavior acting by turbulent surface layer. Combined DIMM and MASS data with microthermal C_T^2 measurements, we can predict atmospheric conditions above the site and we evaluate characteristic at the site. Microthermal C_T^2 measurements can define the height of the telescope finally.

Acknowledgements

We express much thanks to staff members for the site survey project in west China at Kashi and Karasu during preparation, installation and operations of the CT2 system. We also express deep thanks to Dr. Ikuru Iwata for his collaborations on comparison of C_T^2 measurements with the OAO sensor system and our system. Prof. Hiroyasu Ando has given his continuous encouragement and supports to our project. Heiwa-Nakajima foundation is very much appreciated for their support to our project in 2007.

References

Bufton, J. L., 1973, Journal of the Atmospheric Sciences, 30, 83-87,
"Correlation of Microthermal Turbulence Data with Meteorological Soundings in the Troposphere".

Coulman, C. E., 1985, Ann. Rev. Astron. Astrophys., 23, 19-57,
"Fundamental and Applied Aspects of Astronomical “Seeing” ".

Erasmus, D. A. 1986, PASP, 98, 254,
"Meteorological Conditions Affecting Observing Quality on Mauna-Kea".

Erasmus, D. A. and Thompson L. A., 1986, SPIE 628, 148-155,
"Ground turbulence at Mauna Kea Observatory: Location and ground height for future telescopes"

Fried, D. L., 1982, JOSA, 72, 52-61,
" Anisoplanatism in adaptive optics"

Kolmogorov, A.N., 1941, Dokl. Acad. Nauk SSSR, 30, 9 (reprinted in Proc. R. Soc. Lond., A 434, 9, 1991),
"The local structure of turbulence in incompressible viscous fluid for very large Reynolds number".

Kunkel, K. E. & Walters, D. L., 1981, J. App. Meteorology, 20, 130-136,
"Behavior of the Temperature Structure Parameter in a Desert Basin".

Lynds, C. R., 1964, IAU Symposium 19 (ed. Jean Rosch, Gauthier-Villars, Paris), 126-131,
"Observations on microthermal turbulence"

Martin F., Conan, R., Tokovinin, A., Ziad, A., Trinquet, H., Borgnino, J., Agabi, A., & Sarazin, M., 2000, A. A. Suppl., 144, 39-44,
"Optical parameters relevant for High Angular Resolution at Paranal from GSM instrument and surface layer contribution".

Miyashita, A., Noguchi, T. , Yamashita, Y. , Nishimura, S., Tanabe, H. , Ando, Y. , Nariai, K. & Hayashi, S. 1989, Rep.NAOJ, 1, 61-70 (in Japanese),
"Astronomical Evaluation of Mauna Kea for JNLT site"

Roddier, F. 1999, in Adaptive Optics in Astronomy (ed. F. Roddier, Cambridge Univ. Press), 9-22,
"Imaging through the atmosphere"

Sanchez, L. J., Cruz, D. X., Avila R., Agabi, A., Azouit, M., Cuevas, S., Garfias, F., Gonzalez, S. I., Harris, O., Masciadri, E., Orlov, V. G., Vernin, J. & Voitsekhovich V. V., 2003, Rev. Mex. A. A., 19, 23-30,
"Contribution of the Surface Layer to the Seeing at San Pedro Martir: Simultaneous Microthermal and DIMM Measurements".

Sasaki, T., 2008, "Notes on analyses of FriOWL and CLAUS weather database", private communication.

Wada, S., Maihara, T., Hirata, R., Ohta, K., Iwamuro, F., Iwata, I., Kimura, M., Eto, S., Ando, M., Shimono, A., Koyano, H., Yoshida, M., Okita, K., Okada, T., Izumiura, H., Shimizu, Y., Inata, M., Yanagisawa, K., Nagayama, S., Hattori, T., Tamura, N. & Mikami, Y., 2004, Rep. NAOJ, 7, 29-39 (in Japanese),
"Astronomical Evaluation of OAO: Site Research on Surface Boundary Layer of Air"

Woolf , N. J. 1982, Ann. Rev. Astron. Astrophys., 20, 367-398,
"High Resolution Imaging From the Ground".

Wyngaard, J. C. Izumi, Y., and Collins, S. A. Jr., 1971, J. Opt. Soc. Am, 61, 1646-1650,
"Behavior of the Refractive-Index -Structure Parameter near the Ground".

Appendix

A-1. Refractive index structure coefficient, temperature structure coefficient, and seeing size

The fluctuation in the refractive index of the air above the telescope affects the light path to degrade image of stars. A structure function for the refractive index, $D_n(r)$, is defined as

$$D_n(r) = \langle |n(x)-n(x+r)|^2 \rangle, \quad \text{(A1)}$$

where the angle bracket denote an average (Coulman 1985). For locally isotropic turbulent fields, the one-dimensional structure function has the form

$$D_n(r) = C_n^2 \, r^{2/3}, \quad \text{(A2)}$$

where C_n^2 is the refractive index structure coefficient (Kolmogorov 1941). Experimentally, the power law in Eq. A2 has been found to be quite accurate over distances less than 1 meter (Roddier 1999).

The refractive index fluctuation is related to its thermal fluctuations. The refractive index variations arise from density variations in the air. Assumed that fluctuations are passive under the constant pressure, the refractive index variations arise directly from temperature fluctuations and can be measured by using the temperature fluctuations (Woolf 1982) with

$$C_n^2(z) = (7.9\ 10^{-5} \cdot P / T^2)^2 \, C_T^2(z), \quad \text{(A3)}$$

where C_n^2 is the refractive index structure coefficient, and C_T^2 the temperature structure coefficient. Pressure P is in hPa, temperature T in K degree (Erasmus & Thompson 1986), and z is height above the ground in meter.

A blurred image or seeing size is obtained by integrating the refractive index fluctuations along light path (Woolf 1982). A wavelength-dependent length r_0, Fried's parameter (Fried 1982), is

$$r_0(\lambda) = 0.184 \, \lambda^{6/5} \, (\cos\gamma)^{3/5} \, [\int_z^\infty C_n^2(z)\, dz]^{-3/5}, \quad \text{(A4)}$$

where λ is the wavelength in meter and γ the zenith distance. We are considering the seeing toward the zenith, cos γ is unity. As a seeing size θ (radian) is evaluated at full width at half maximum,

$$\theta(z) = 0.98 \, (\lambda / r_0(\lambda)) . \quad \text{(A5)}$$

Then we obtain by substituting the equation (A4) to (A5),

$$\theta(z) = 5.3 \, \lambda^{-1/5} [\int_z^\infty C_n^2(z)\, dz]^{3/5}. \quad \text{(A6)}$$

With the equation (A3), we obtain the seeing size using temperature structure coefficient, C_T^2, as

$$\theta(z) = 5.3 \, \lambda^{-1/5} (7.9\ 10^{-5} \cdot P / T^2)^{6/5} [\int_z^\infty C_T^2(z)\, dz]^{3/5}. \quad \text{(A7)}$$

The temperature structure coefficient, C_T^2, is defined like C_n^2 in equations (A1) and (A2) as

$$C_T^2 = \langle |T(x)-T(x+r)|^2 \rangle \cdot r^{-2/3} \quad (K^2 m^{-2/3}), \quad \text{(A8)}$$

where r is a separation of two temperature sensors. In the case of stratified air, a vertical distribution of C_T^2 is observed in exponential form with exponential scale height z_h as

$$C_T^2(z) = C_T^2(0) \exp (-z / z_h), \quad \text{(A9)}$$

where $C_T^2(0)$ is the value at the ground level z=0. Substituting the equation (A9) to (A7) and integrating, we obtain seeing at z as

$$\theta(z) = 5.3 \, \lambda^{-1/5} (7.9\ 10^{-5} \cdot P / T^2)^{6/5} \cdot (C_T^2(0) \cdot z_h \cdot \exp(-z / z_h))^{3/5} \quad \text{(radian)}, \quad \text{(A10)}$$

$$= 5.3 \, \lambda^{-1/5} (7.9\ 10^{-5} \cdot P / T^2)^{6/5} \cdot (C_T^2(z) \cdot z_h)^{3/5} \quad \text{(radian)}, \quad \text{(A11)}$$

and the seeing at the ground level

$$\theta(0) = 5.3 \, \lambda^{-1/5} (7.9\ 10^{-5} \cdot P / T^2)^{6/5} \cdot (C_T^2(0) \cdot z_h)^{3/5} \quad \text{(radian)}. \quad \text{(A12)}$$

A-2. Conversion factor to C_T^2 values from rms of differential voltages of paired CT2 sensors

The temperature dependence of thin nickel wire was measured in the Laboratory at Mitaka. A resistance of the wire spiraled to CT2 sensors (1.9m long) is measured of 245.225Ω, 252.73Ω, 282.75Ω at different temperatures, -5, 0 and 20 ℃, respectively. The resistance dependency on temperature, C_t, is obtained of 1.501Ω/℃. Then resistance of the nickel wire, $R_{NI,}$ is described as

$$R_{NI}(T) = C_t (T(K) - 273.15) + R_{273}\,,$$

(A13)

where temperature in K degree and R_{273} is the resistance of the nickel wire at 0 ℃, measured as 252.73Ω.

As a pair of CT2 sensors constitute a part of a Wheatstone bridge circuit with additional 1.5KΩ, 200Ω adjustable resistance and 1.62KΩ (Figure 5). When one of paired sensors has a different temperature from the other by ΔT, the combined resistance R_C is calculated as

$$R_C(T, \Delta T) = R_A(T)\, R_B(T+\Delta T) / (R_A(T) + R_B(T+\Delta T)),$$

(A14)

where $R_A(T) = R_{NI}(T) + R_D$, $R_B(T+\Delta T) = R_{NI}(T+\Delta T) + R_D$, and constant resistance R_D = 1620Ω in the Wheatstone bridge. A constant voltage V_C of 7.5 V is supplied to the bridge circuit, the current is $I_C(T, \Delta T) = V_C / R_C(T, \Delta T)$, depending on the temperature. The currents through each sensor are calculated as $I_A = I_C R_B / (R_A + R_B)$ and $I_B = I_C R_A / (R_A + R_B)$. Then the voltage difference between the CT2 sensors is

$$\Delta V(T, \Delta T) = I_A R_A - I_B R_B\,,$$

(A15)

which under the conditions of $\Delta T \ll 1$ is nearly equal to

$$\Delta V(T, \Delta T) \approx -V_C R_D C_t \Delta T / (R_{273} + C_t (T(K) - 273.15) + R_D)^2.$$

(A16)

Then

$$\Delta V / \Delta T = -V_C R_D C_t / (R_{273} + C_t (T(K) - 273.15) + R_D)^2.$$

As C_T^2 is defined in equation (A8) and a separation of paired CT2 sensor, r meter, a conversion factor, f_{conv}, to a C_T^2 value from the voltage difference ΔV is obtained under voltage amplification of 1000 as

$$f_{conv}(T) = (1000 \times \Delta V / \Delta T)^{-2} r^{-2/3},$$
$$= (R_{273} + C_t (T(K) - 273.15) + R_D)^4 / (1000\, V_C R_D C_t)^2 / r^{2/3}. \quad (K^2 \quad m^{-2/3} \quad V^{-2})$$

(A17)

Typical values of $f_{conv}(T)$ are 0.0364, 0.0370, and 0.0394 at -5, 0 and 20 ℃, respectively, with r=1 meter in our case. Taking into account an offset voltage, V_{offset}, by AD536ASD, then we obtain C_T^2 values from an output V_{rms} of AD536ASD as

$$C_T^2 = f_{conv}(T, \Delta T) \times (V_{rms} - V_{offset})^2. \quad \text{(A18)}$$

A-3. Computer Software used

A-3-1. ContCT2

Control software to get microthermal data with conversion to microthermal values from voltage taken with Keithley DMM. Values of microthermal measurements, temperature, and atmospheric pressure are displayed in real-time.

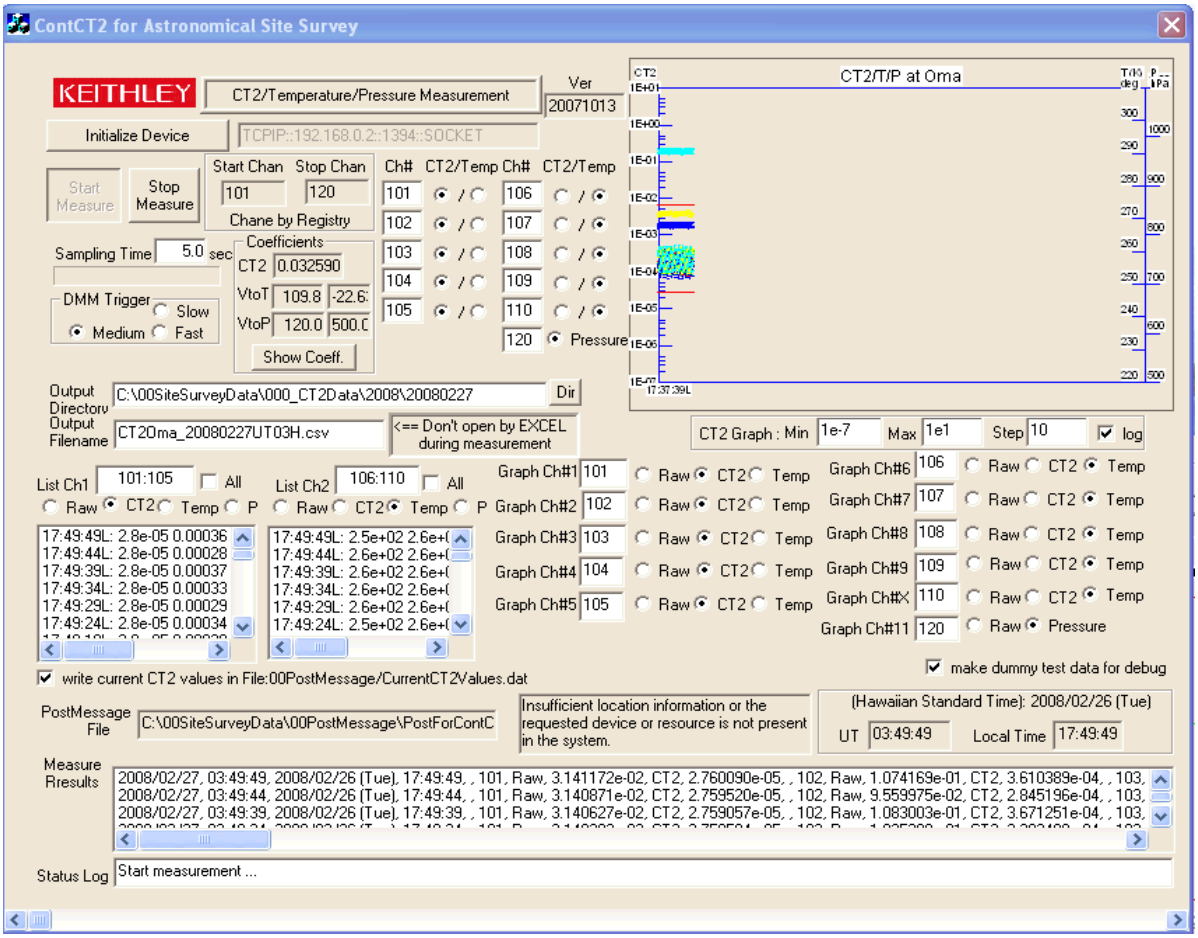

Drivers used for Keithley Digital Multimeter (DMM) should be installed about three exe files below.

Keithley2700-851B03.exe (44 MB)
Keithley2700-852B01_4.exe (9 MB)
KeithleyIOLayerB05.exe (47 MB)

Input: connected to Keithley Digital Multimeter (DMM) via Ethernet.

Output: measured values of CT2, temperatures, and atmospheric pressure with raw voltage and converted values, saved in file:

C:¥ 00SiteSurveyData¥000_CT2Data¥mmyydd¥mmyydd¥ CT2Karasu_20071028UT00H.csv

An output file name is changed automatically every hour.

Windows system registries are used in [HKEY_CURRENT_USER¥Software¥ToshiWare¥ContCT2Dlg¥CT2Control]

"ContCT2_Version"="20071013"
"Location"="Karasu"
"CopyRight"="ToshiWare/NAOJ 2007"
"DMMChannels"="101:120"
"DMM_ComMode"="TCPIP::192.168.0.2::1394::SOCKET"
"PostMessageFile"="C:¥¥00SiteSurveyData¥¥00PostMessage¥¥PostForContCT2.txt"
"SamplingTime"="5.0"
"CoefficientVtoCT2"="0.032590122"

"CoefficientVtoT"="1.0"
"CoefficientVtoP"="120"
"OffsetVforT"="0.0"
"OffsetVforP"="500"
"Port1"="101"
"Port2"="102"
"Port3"="103"
"Port4"="104"
"Port5"="105"
"Port6"="106"
"Port7"="107"
"Port8"="108"
"Port9"="109"
"PortX"="110"
"Port11"="120"
"GraphCh1"="101"
"GraphCh2"="102"
"GraphCh3"="103"
"GraphCh4"="104"
"GraphCh5"="105"
"GraphCh6"="106"
"GraphCh7"="107"
"GraphCh8"="108"
"GraphCh9"="109"
"GraphChX"="110"
"GraphCh11"="120"
"GraphCT2_Min"="1e-6"
"GraphCT2_Max"="1e0"
"GraphCT2_Step"="10"
"GraphTemp_Min"="220"
"GraphTemp_Max"="310"
"GraphTemp_Step"="10.0"
"GraphPressure_Min"="500.0"
"GraphPressure_Max"="1100.0"
"GraphPressure_Step"="100.0"
"RawVolt_Min"="0.0"
"RawVolt_Max"="10.0"
"OutDirectory"="C:¥¥00SiteSurveyData¥¥000_CT2Data¥¥2008¥¥20080129"
"MaxListBoxLines"="1000"
"OutFilename"="CT2Karasu_20080129UT00H.csv"
"GraphCT2_Log"="1"
"ListChannel1"="101:105"
"ListChannel2"="106:110"
"List1Mode"="1"
"List2Mode"="2"
"List1All"="0"
"List2All"="0"
"GraphCh1Mode"="1"
"GraphCh2Mode"="1"
"GraphCh3Mode"="1"

"GraphCh4Mode"="1"
"GraphCh5Mode"="1"
"GraphCh6Mode"="2"
"GraphCh7Mode"="2"
"GraphCh8Mode"="2"
"GraphCh9Mode"="2"
"GraphChXMode"="2"
"GraphCh11Mode"="1"
"Port1Mode"="0"
"Port2Mode"="0"
"Port3Mode"="0"
"Port4Mode"="0"
"Port5Mode"="0"
"Port6Mode"="1"
"Port7Mode"="1"
"Port8Mode"="1"
"Port9Mode"="1"
"PortXMode"="1"
"Port11Mode"="0"
"DMMTrigger"="0"
"ChScale1"="0.032590122"
"ChScale2"="0.032590122"
"ChScale3"="0.032590122"
"ChScale4"="0.032590122"
"ChScale5"="0.032590122"
"ChScale6"="103.2"
"ChScale7"="103.1"
"ChScale8"="103.3"
"ChScale9"="103.0"
"ChScale10"="104.0"
"ChScale11"="120.0"
"ChOffset1"="0.00186"
"ChOffset2"="0.00150"
"ChOffset3"="0.00152"
"ChOffset4"="0.00172"
"ChOffset5"="0.00152"
"ChOffset6"="0.0"
"ChOffset7"="0.0"
"ChOffset8"="0.0"
"ChOffset9"="0.0"
"ChOffset10"="0.0"
"ChOffset11"="500.0"
"SaveCurrentValuesInFile"="1"

A-3-2. CT2ToSeeing

To estimate seeing size induced by surface atmospheric turbulence from microthermal values taken with ContCT2. Conversion of seeing is carried out in real time or for stored data in files by selecting analysis mode.

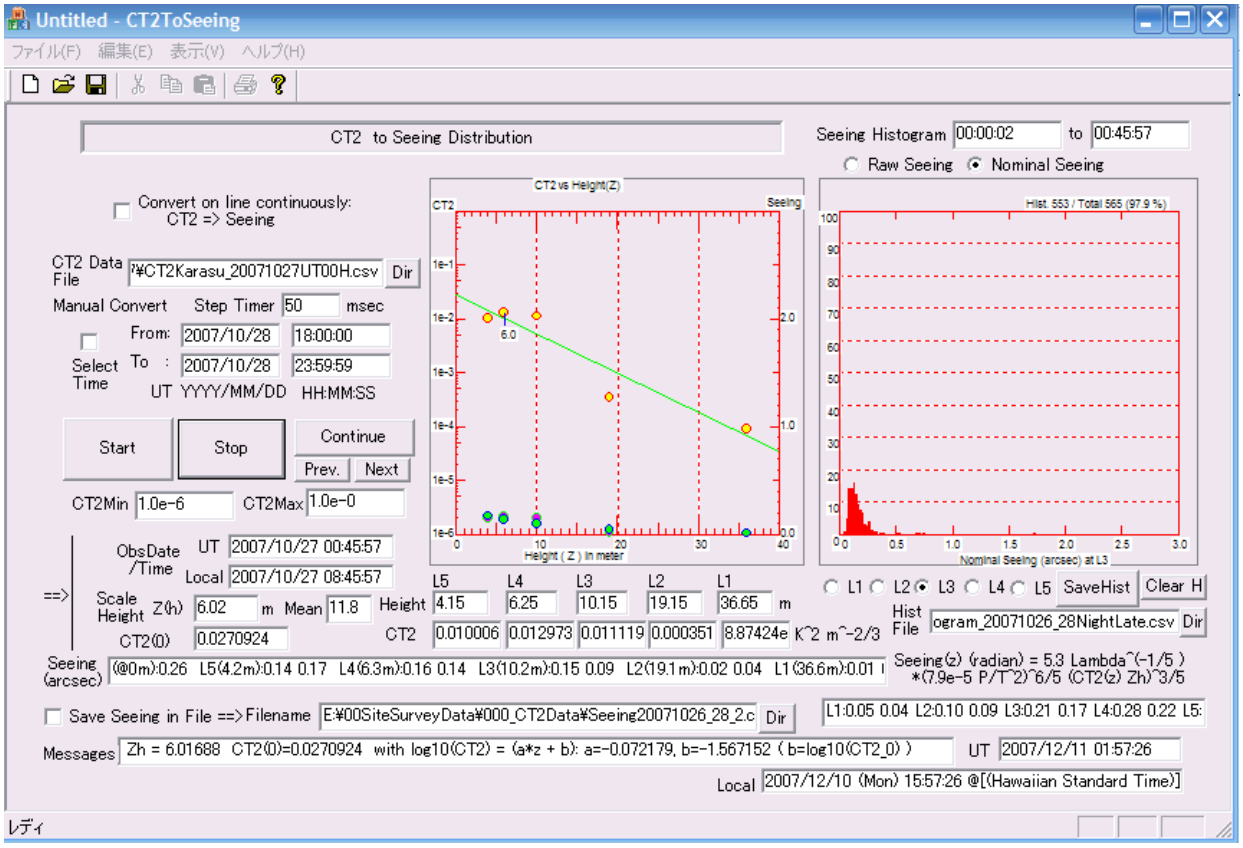

Input: from real-time data saved in file: (default) C:¥00SiteSurveyData¥00PostMessage¥CurrentCT2Values.dat

Off-line analysis on data in file : (default)

C:¥00SiteSurveyData¥000_CT2Data¥yyyymm¥mmmmyydd¥CT2Karasu_20071028UT00H.csv

Output: Seeing data obtained are saved in file:

C:¥ 00SiteSurveyData¥000_CT2Data¥Analysis_20071026_28¥Seeing20071026_28.csv

Seeing histogram obtained is saved in file with manual operation:

C:¥ 00SiteSurveyData¥000_CT2Data¥Analysis_20071026_28¥CT2ToSeeingHistogram.csv

Windows system registries are used in

[HKEY_CURRENT_USER¥Software¥ToshiWare¥CT2ToSeeing¥CT2ToSeeing]

"CT2Filename"="C:¥¥00SiteSurveyData¥¥000_CT2Data¥¥CT2Karasu_20071026_28.csv"

"CT2Directory"="C:¥¥00SiteSurveyData¥¥000_CT2Data"

"CT2Max"="1"

"CT2Min"="1e-6"

"CT2Level1"="36.65"

"CT2Level2"="19.15"

"CT2Level3"="10.15"

"CT2Level4"="6.25"

"CT2Level5"="4.15"

"DisplaySeeingMin"="0.0"

"DisplaySeeingMax"="1.5"

"HistDirectory"="C:¥¥00SiteSurveyData¥¥000_CT2Data"

"HistFilename"="C:¥¥00SiteSurveyData¥¥000_CT2Data¥¥CT2ToSeeingHistogram2.txt"
"StepTimer"="50"
"AutoConvert"="0"
"StartDate"="2007/10/12"
"StartTime"="00:00:00"
"EndDate"="2007/10/12"
"EndTime"="23:59:59"
"OutFilename"="C:¥¥00SiteSurveyData¥¥000_CT2Data¥¥Seeing20071026_28_2.csv"
"OutDirectory"="C:¥¥00SiteSurveyData¥¥000_CT2Data"
"SaveSeeingInFile"="1"
"LevelForHistogram"="0"
"DisplaySeeingStep"="0.02"
"HistogramFromRaw"="0"

A-3-3. CT2Graph

To make Postscript file to draw CT2 measurements values and optionally to convert the PS file to PDF format using Adobe AcrobatDistriller. PDF files can be shown using Adobe AcroRead. For real time use, a file conversion is carried on automatically in a certain period after the change of CT2 file timestamp is ceased. Automated creation of back up files for the CT2 files are planned to be optional to any directory (created if it is a new directory) (NOT completed).

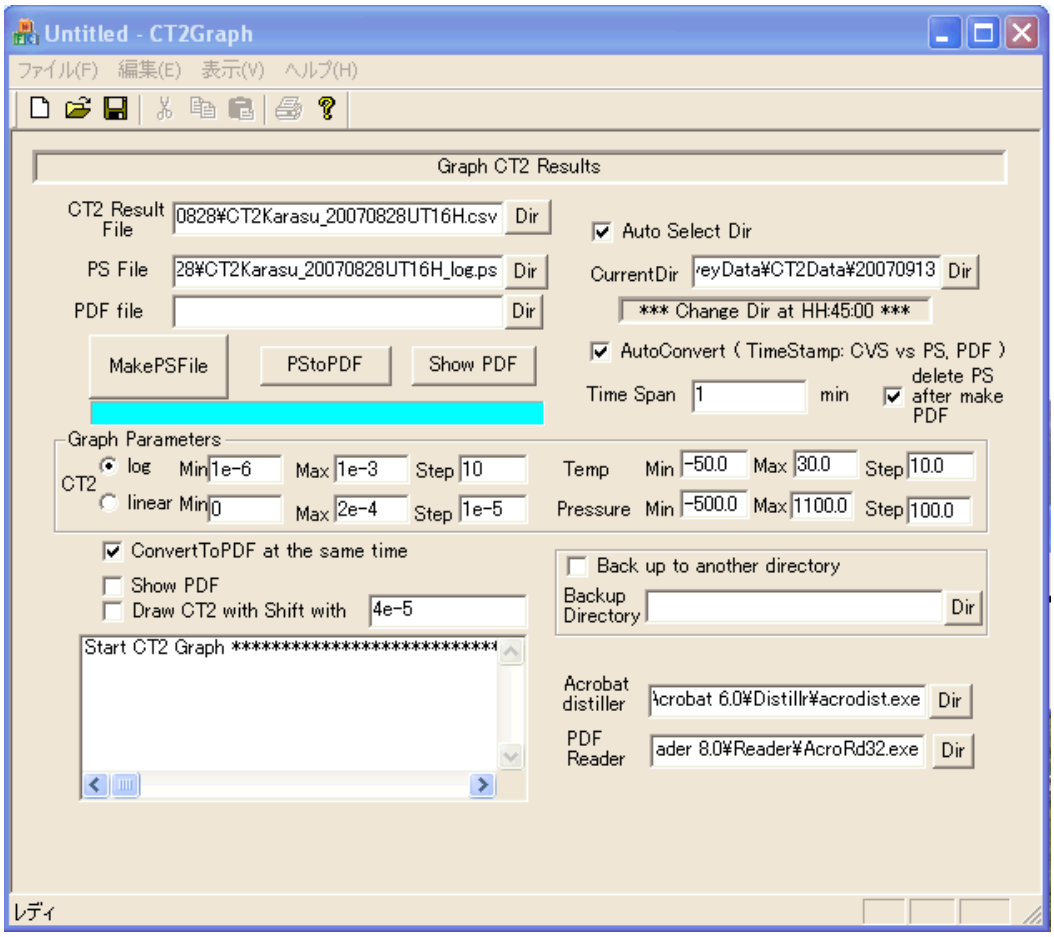

Input: CT2 file: (default) C:¥00SiteSurveyData¥00PostMessage¥CurrentCT2Values.dat
Output: Postscript file created by CT2Graph in any directory:

ex) C:¥00SiteSurveyData¥CT2Data¥20070828¥CT2Karasu_20070828UT16H_log.ps

PDF file converted from Postscript file using Adobe Acrobat Distrill in the same directory of the PS file:

ex) C:¥00SiteSurveyData¥CT2Data¥20070824¥CT2Karasu_20070824UT16H_log.pdf

Windows system registries are used in [HKEY_CURRENT_USER¥Software¥ToshiWare¥CT2Graph¥CT2Graph]

"AcroDistFilename"="C:¥¥Program Files¥¥Adobe¥¥Acrobat 6.0¥¥Distillr¥¥acrodist.exe"
"AcroReaderFilename"="C:¥¥Program Files¥¥Adobe¥¥Reader 8.0¥¥Reader¥¥AcroRd32.exe"
"DrawShiftValue"="4e-5"
"TimeSpan"="1"
"CT2Directory"="C:¥¥00SiteSurveyData¥¥CT2Data¥¥20070828"
"CT2Filename"="C:¥¥00SiteSurveyData¥¥CT2Data¥¥20070828¥¥CT2Karasu_20070828UT16H.csv"
"PSDirectory"="C:¥¥00SiteSurveyData¥¥CT2Data¥¥20070828"
"PSFilename"="C:¥¥00SiteSurveyData¥¥CT2Data¥¥20070828¥¥CT2Karasu_20070828UT16H_log.ps
"
"PDFDirectory"="C:¥¥00SiteSurveyData¥¥CT2Data¥¥20070828"
"PDFFilename"="C:¥¥00SiteSurveyData¥¥CT2Data¥¥20070828¥¥CT2Karasu_20070828UT16H_log.
pdf"
"AutoSelectedDirectory"="C:¥¥00SiteSurveyData¥¥CT2Data¥¥20070913"
"SimultaneousConvertToPDF"="1"
"ShowPDF"="0"
"DrawWithShift"="0"
"LogMin"="1e-6"
"LogMax"="1e-3"
"LogStep"="10"
"LinearMin"="0"
"LinearMax"="2e-4"
"LinearStep"="1e-5"
"LogScale"="0"
"TempMin"="-50.0"
"TempMax"="30.0"
"TempStep"="10.0"
"PressureMin"="-500.0"
"PressureMax"="1100.0"
"PressureStep"="100.0"
"AutoDirChange"="1"
"AutoConvertToPDF"="1"
"DelPSAfterPDF"="1"
"BackupDirectory"=""

---- End of the Document -----